Development of Single Layer of WO_3 on Large Spatial Resolution by Atomic Layer Deposition Technique

S. Zhuiykov, Zh. Hai, H. Xu, C. Xue

***Abstract*—**Unique and distinctive properties could be obtained on such two-dimensional (2D) semiconductor as tungsten trioxide (WO_3) when the reduction from multi-layer to one fundamental layer thickness takes place. This transition without damaging single-layer on a large spatial resolution remained elusive until the atomic layer deposition (ALD) technique was utilized. Here we report the ALD-enabled atomic-layer-precision development of a single layer WO_3 with thickness of 0.77±0.07 nm on a large spatial resolution by using $(^tBuN)_2W(NMe_2)_2$ as tungsten precursor and H_2O as oxygen precursor, without affecting the underlying SiO_2/Si substrate. Versatility of ALD is in tuning recipe in order to achieve the complete WO_3 with desired number of WO_3 layers including monolayer. Governed by self-limiting surface reactions, the ALD-enabled approach is versatile, scalable and applicable for a broader range of 2D semiconductors and various device applications.

***Keywords*—**Atomic layer deposition, tungsten oxide, WO_3, two-dimensional semiconductors, single fundamental layer.

I. Introduction

NEWLY discovered properties of 2D semiconductors allowed them to be incorporated onto mechanically conformal platforms, which in return, provides unprecedented pathway for development of stretchable complex electronic devices which could be twisted, stretched or folded and unfolded without losing their major characteristics, reliability, durability and performance. Among recently developed transition 2D metal oxide semiconductors, WO_3 has been successfully utilized in optical switches [1], batteries [2], electro-chromic (smart windows) [3], various chemical gas sensors [4], [5], solar cells [6], catalytic [7], and photo-catalytic [8] applications. The interest to further modification of this semiconductor has been strikingly highlighted over the past few years with the possibility of making WO_3 in 2D form, which clearly exhibited the modulation of bandgap [9]. However, most of the published results for 2D semiconductors are related only to 2D nano-structures developed on small areas either by mechanical [10] or by liquid exfoliation techniques [11]. Furthermore, exfoliated 2D films sometimes contain non-uniform domains with different numbers of layers [12]. Although 2D WO_3 nanocrystals obtained so far have shown great properties and performance, to the best of our knowledge, there were no reports about development of a single layer 2D WO_3 across a large area with precise control of deposition rate and parameters.

ALD, as a variant of the CVD technique, is a deposition technique based on a series of self-limiting, surface-saturated reactions to form thin conformal films at a controllable rate [13]. However, only few ALD processes have been reported so far for fabrication of thin-film WO_3 [14].

In this paper, we report the ALD-based synthesis of WO_3 monolayers, with excellent uniformity and thickness tenability across 4 inch wafers. Single layer of WO_3 with thickness of ~0.77±0.07 nm has been developed on a large scale by using $(^tBuN)_2W(NMe_2)_2$ as tungsten precursor and H_2O as oxygen precursor.

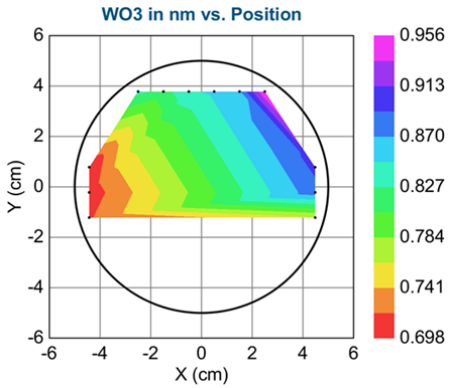

Fig. 1 Ellipsometry data for the single-layered WO_3 after final recipe correction

The experimental data for both H_2O and $(^tBuN)_2W(NMe_2)_2$ precursors were in agreement with a surface adsorption model (Langmuir model). It is evident that the growth is self-limiting. Noteworthy the optimum H_2O pulse time 40-100 ms is longer than what is used in typical oxide growths in a Savannah system, but was found necessary. The slow oxidation of $(^tBuN)_2W(NMe_2)_2$ is appeared to be responsible for the shorter H_2O pulses (e.g., 10 ms). In addition, it was established that the growth was also highly sensitive to the substrate temperatures. The first deposition at operating temperature of ~ 300 °C confirmed that very limited growth of

S. Zhuiykov is with the Gent University Global Campus, Incheon, 406-840, South Korea (corresponding author phone: +82-32-626-4209; fax: +82-32-626-4109; e-mail: serge.zhuiykov@ugent.be).
Zh. Hai is with the Gent University Global Campus, Incheon, 406-840, South Korea (e-mail: zhenyin.hai@ugent.be).
H. Xu is with School of Materials Science and Engineering, North University of China, 030051, P.R. China (e-mail: xuhongyan@nuc.edu.cn).
C. Xue is with Key Laboratory of Instrumentation Science and Dynamic Measurement of Ministry of Education, North University of China, 030051, P.R. China (e-mail: xuechenyang@nuc.sdu.cn).

the WO_3 film was obtained. In total seven depositions were performed, each with corresponding ellipsometry measurement, analysis and further optimization. Thus, the optimum growth conditions were found as follows: $[(^tBuN)_2W(NMe_2)_2$ pulse 2 s, N_2 purge 10 s, H_2O pulse 50 ms, N_2 flow 5 s without pumping and then 10 s with pumping, T=350 °C yielded stable WO_3 growth. Therefore, final single layer 2D WO_3 films were developed on 4" SiO_2/Si substrates with deposited Au/Cr electrodes after optimization of the established recipe. Subsequent ellipsometry analysis of the final deposition (Fig. 1) has indicated that the obtained 2D WO_3 ultra-thin films were 0.77 ± 0.07 nm and indeed represented a single fundamental layer of WO_3. These data were collected at the exterior of the wafer on the bare parts of the silicon that had no Au/Cr coating. Considering that the roughness of the standard silicon wafer is about ± 0.5 nm, it was hard to establish more consistent ALD monolayer WO_3 deposition with less than 10% variation. Thus, new ALD recipe for the development of a single fundamental layer of WO_3 introduced in this work presents good overall deposition characteristics.

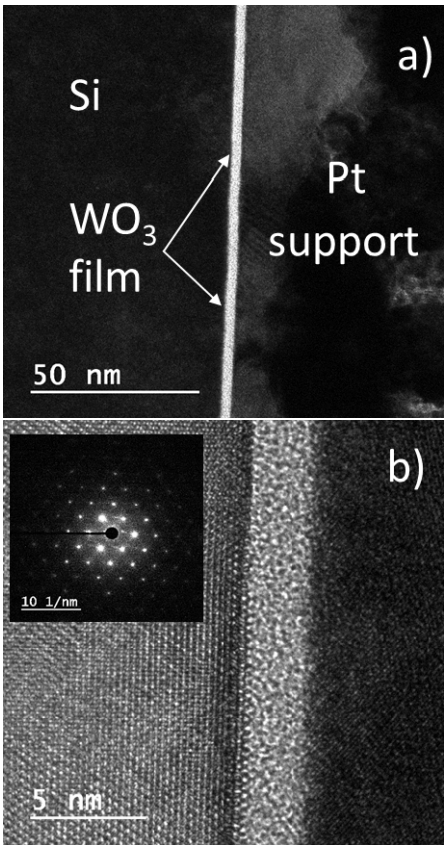

Fig. 2 (a) STEM cross-sectional view of ~3.3 nm thick 2D ALD-deposited WO_3 film (b) High-magnification of the interface between Si wafer and WO_3 film. Insert shows the SAED pattern indicating crystalline structure of Si

Scanning Transmission Electron Microscopy (STEM) analysis was involved for measurement slightly thicker 2D WO_3 (~3.3 nm). The intention to developed thicker 2D WO_3 (~3.3 nm) film for the cross-sectional cut by FIB-SEM because it was impossible to make similar sample for STEM analysis consisting only of monolayer WO_3 film. The nature of the FIB was quite aggressive, which resulted in damaging all ALD-deposited monolayer WO_3 samples during the cuts, even though platinum (Pt) was sputtered on the top of WO_3 to make the rigid supporting layer before the cross-sectional cut. Only when the thickness of 2D WO_3 was increased to ~3.3 nm, the overall structure became stable. It is clear from the presented STEM image that the ALD-deposited WO_3 film was uniform across a large area of Si wafer and was amorphous without clearly identified crystalline structure, as depicted in the high-magnification STEM image in Fig. 2 (b).

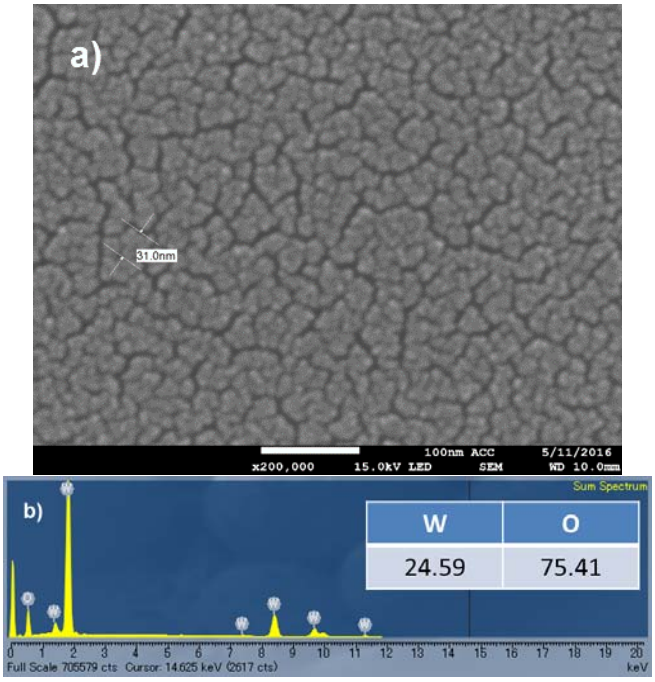

Fig. 3 (a) SEM image of the surface morphology of monolayer WO_3 film annealed at 200 °C with measurement of the average grains' size (b) EDX spectra for annealed WO_3 film

Fig. 3 (a) depicts typical SEM image of the surface of annealed WO_3 film. The silicon substrate was completely covered by WO_3 and no cracks and/or surface agglomerations of WO_3 grains were observed. Instead the surface morphology of ALD-developed WO_3 film represents uniform structure with the average WO_3 grains size varying from 30 nm to approximately 60 nm in lengths, as measured by SEM apparatus. Further observation of the local chemical homogeneity of monolayer WO_3 films by EDX indicated that the developed films were stoichiometric with no impurities observed in EDX spectra (Fig. 3 (b)).

Following the STEM, SEM and EDX analysis, electronic structure and chemical composition of single layer WO_3 films were analyzed by XPS technique. The decomposition of W 4f and O 1s spectra was carried out by Gauss-Newton method. The area of all peaks was determined after subtraction of background by Shirley method. Fig. 4 (a) depicts the XPS

survey wide scan spectra for 2D WO_3 films. The C 1s peak at 284.6 eV, which originates from the surface adsorbed carbon species, is used for calibration purpose. It was found that no impurity was contained on ultra-thin 2D WO_3 surfaces, and peaks were consisted only of W, O, and Si, respectively. The detailed core-level spectra of W 4f and O 1s peaks for both 2D WO_3 films are presented in Figs. 4 (b) and (c), respectively. The detailed core-level spectra for W $4f_{7/2}$ peaks at 36.2 eV and 35.2 eV in this work represent W 4f peaks of WO_3.

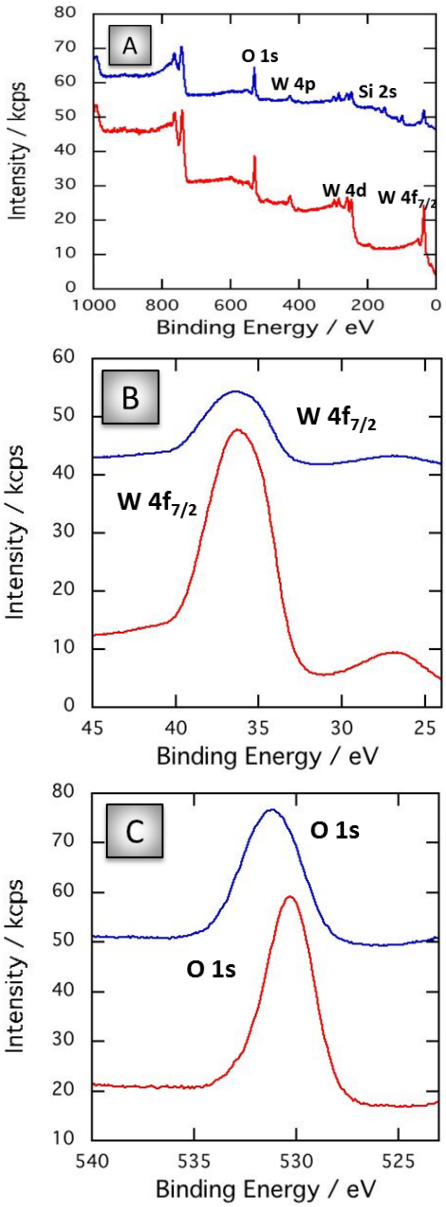

Fig. 4 (a) XPS Spectra of wide scan, (b) W 4f and (c) O 1s scans, respectively; Blue and red lines are single-layered and 10.0 nm-thick WO_3 samples, respectively

The energy position of the main peaks corresponded to the W^{6+} state. Noteworthy, the integrated peak area suggested that the amount of W in WO_3 film sample with thickness of ~10.0 nm and its intensity was approximately 3.2 times larger than that in the single layer WO_3 film sample. The difference between W $4f_{7/2}$ peaks for ~10.0 nm and >1.0 nm thick WO_3 films is reasonable considering that the amount of W in the first and second samples, respectively. However, the recorded W $4f_{7/2}$ peaks position for both ALD-developed WO_3 ultra-thin films is slightly different than that for W $4f_{7/2}$ peaks measured for sputtered thin-film WO_3 (W $4f_{7/2}$ = 34.35 eV) [15], WO_3 nanoparticles sintered at 280 °C (W $4f_{7/2}$ = 35.83 eV) and for WO_3 micro-spheres (W $4f_{7/2}$ = 34.50 eV) [16]. It should be also noted that no W $4f_{5/2}$ peaks were observed.

The maximum of O 1s peaks for both WO_3 samples was observed at 532.0 eV and 530.5 eV, respectively, as presented in Fig. 4 (c). These peaks corresponded to O 1s-levels of oxygen atoms O^{2-} in the lattice of SiO_2 and WO_3 [17]. Lattice constants of oxygen-octahedron of WO_3 are calculated to be a = 7.31 Å and b = 7.54 Å, respectively. The position of O 1s peaks for the ALD-developed ultra-thin WO_3 films was similar to the O 1s peaks recorded for WO_3 thin-films developed by sol-gel technique (O 1s = 530.5eV) [18]. If the thickness of ultra-thin 2D WO_3 sample was consisted of double layer of oxygen-octahedron structure, the bottom oxygen is shared with SiO_2. XPS spectra depicted that oxygen of 6 layers of oxygen-octahedron structure in the 10.0 nm-thick WO_3 sample is totally free from the substrate effect.

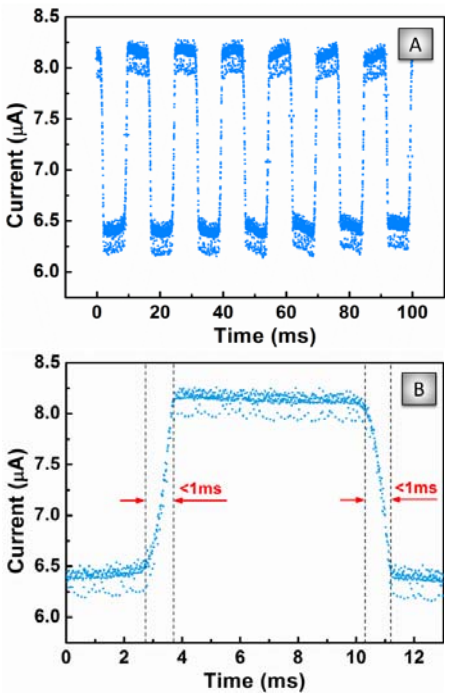

Fig. 5 (a) Time-resolved photo-response of monolayer WO_3 under 360 nm UV illumination (b) Response time of WO_3 film under 360 nm illumination

Owing to wide bandgap single-layered WO_3 films were utilized in UV photodetectors. In order compare the performance of modern photodetectors reported to date, both repeatability and repose time of the monolayer WO_3-based photodetector were tested because these two parameters are the key parameters determining the capability of

photodetectors. Until now it is still a challenge to achieve photodetectors with both high sensitivity and fast temporal response. Fig. 5 depicts the performance of the monolayer WO_3-based photodetector under λ=360 nm illumination. The results obtained shown that the device mostly exhibited two distinct states, a low-current state of ~6.45 μA in the dark and high-current state of ~8.3 μA under λ=360 nm light illumination. The current increases very rapidly from one state to another, indicating a very fast speed of the device. The measured response time was less than ~1.0 ms, which confirmed significantly enhanced performance of monolayer WO_3-based device compared with that of other reported photodetectors based on WO_3 nanosheets (80 ms), nanowire (>50 s) [19], thin films (>47 ms) [20], bilayer ZnS/ZnO (<0.3 s) [21] and monolayer MoS_2 (50 ms) [22]. Consequently, the developed recipe for ALD of monolayer WO_3 has been demonstrated to lead to the production of single-layered WO_3 films with superior monodispersed thickness profile of ~0.77±0.07 nm on a large area. The ALD process has utilized $(^tBuN)_2W(NMe_2)_2$ as tungsten precursor and H_2O as oxygen precursor, respectively, without affecting the underlying SiO_2/Si substrate. Newly developed recipe for the ALD-enabled WO_3 films is presented at the deposition temperature of 350 °C and the process yields pure, stoichiometric single-layered WO_3 films. As-deposited all films were very smooth with uniformed grain sizes distribution. The films' crystallinity and their properties could be further improved by post-deposition annealing in air. Detailed analysis revealed that the produced single-layered WO_3 films are stoichiometric as evident in the XPS spectra with consistent crystalline structure and grain size from ~30 to ~60 nm, evidence by SEM analysis. Prototype of UV photodetector based on monolayer WO_3 film has demonstrated superior response time of less than ~1.0 ms, compare to the other nanostructured WO_3, bilayer ZnS/ZnO and monolayer MoS_2-based photodetectors. Further study is underway to develop ultra-fast, sensitive and reliable UV-A photodetector based on monolayer WO_3.

As both the ALD fabrication process and its framework have great compatibility with other emerging 2D semiconductors and conductors such as graphene, further research along these directions could potentially ensure that the single-layered WO_3 films are able to compete against the best 2D semiconductors. As a result, in the context of flexible electronic applications, the single-layered 2D semiconductors with tunable properties enable to develop devices built entirely out of ultrathin, flexible and transparent 2D materials, which provides imperative benefit for optoelectronic, electro-chromic and nano-electronic applications.

ACKNOWLEDGMENT

The work was supported by the Research and Development Program of the Ghent University Global Campus, South Korea. This work was performed in part at the Melbourne Centre for Nanofabrication (MCN) in the Victoria Node of the Australian National Fabrication Facility (ANFF).

REFERENCES

[1] C. G. Granquist, Electrochromic tungsten oxide films: Review of progress 1993-1998, Sol. Energy. Mater Sol. Cells 60 (2000) 201-262.
[2] S. Yoon, S.-G. Woo, K.-N. Jung, H. Song, Conductive surface modification of cauliflower-like WO_3 and its electrochemical properties for lithium-ion batteries, J. Alloys. Comp. 613 (2014) 187-192.
[3] S. H. Lee, R. Deshpandle, P. A. Parilla, K. M. Jones, B. To, A. H. Mahan, A. C. Dillon, Crystalline WO_3 Nanoparticles for Highly Improved Electrochromic Applications, Adv. Mater. 18 (2006) 763-766.
[4] S. Kim, S. Park, S. Park, C. Lee, Acetone sensing of Au and Pd-decorated WO_3 nanorod sensors, Sens. Actuators B: Chem. 209 (2015) 180-185.
[5] S. Zhuiykov, Morphology and sensing characteristics of nanostructured RuO_2 electrodes for integrated water quality monitoring sensors, Electrochem. Comm. 10 (2008) 839-843.
[6] J. Z. Ou et al. Anodic formation of a thick three-dimensional nanoporous WO_3 film and its photocatalytic property, Electrochem. Comm. 27 (2013) 128-132.
[7] D. J. Ham, A. Phuruangrat, S. Thongtem, J. S. Lee, Hydrothermal synthesis of monoclinic WO_3 nanoplates and nanorods used as an electrocatalyst for hydrogen evolution reactions from water, Chem. Eng. J. 165 (2010) 365-369.
[8] A. Labidi, C. Jacolin, M. Bendahan, A. Abdelghani, J. Guerin, K. Aguir, M. Maaref, Impedance spectroscopy on WO_3 gas sensor, Sens. Actuators B: Chem. 106 (2005) 713-718.
[9] S. Zhuiykov, E. Kats, B. Carey, S. Balendhran, Proton intercalated two-dimensional WO_3 nano-flakes with enhanced charge-carrier mobility at room temperature, Nanoscale 6 (2014) 109-133.
[10] K. Kalantar-zadeh, A. Vijayaraghavan, M. H. Ham, H. Zheng, M. Breedon, M. S. Strano, Synthesis of atomically thin WO_3 sheets from hydrated tungsten trioxide, Chem. Mater. 22 (2010) 5660-5666.
[11] E. Nguyen, T. Daeneke, S. Zhuiykov, K. Kalantar-zadeh, Liquid Exfoliation of layered transition metal dichalcogenides for biological applications, Current Prot. Chem. Biol. 8 (2016) 97-108.
[12] S. Balendhran, S. Walia, M. Alsaif, J.Z. Ou, S. Zhuiykov, S. Sriram, M. Bhaskaran, K. Kalantar-zadeh, Field effect biosensing platform based on 2D α-MoO_3, ACS Nano. 7 (2013) 9753-9760.
[13] S. Moitzheim et al. Nanostructured TiO_2/carbon nanosheet hybrid electrode for high-rate thin-film lithium-ion batteries, Nanotechnology. 25 (2014) 504008.
[14] P. Tagtstrm, P. Martersson, U. Jansson, J.-O. Carlsson, Atomic layer epitaxy of tungsten oxide Films using oxyfluorides as metal precursors, J. Electrochem. Soc. 146 (1999) 3139-3143.
[15] M. T. Chang et al. Nitrogen-Doped tungsten oxide nanowires: low-temperature synthesis on Si, and electrical, optical, and field-emission properties, Small. 3 (2007) 658-664.
[16] S. Balaji, Y. Djaoued, A. S. Albert, R.Z. Ferguson, R. Bruning, Hexagonal tungsten oxide based electrochromic devices: spectroscopic evidence for the Li ion occupancy of four-coordinated square windows, Chem. Mater. 21 (2009) 1381-1389.
[17] M. Sze, K. N. Kwok, Physics of semiconductor devices, Wiley, 2006.
[18] J. C. Dupin, D. Gonbeau, P. Vinatier, A. Levasseur, Systematic XPS studies of metal oxides, hydroxides and peroxides, Phys. Chem. Chem. Phys. 2 (2000) 1319-1324.
[19] J. Liu, M. Zhong, J. Li, A. Pan, X. Zhu, Few-layer WO_3 nanosheets for high-performance UV-photodetectors, Mat. Lett. 148 (2015) 184-187.
[20] Juan, Y. M. et al. Self-powered hybrid humidity sensor and dual-band UV photodetector fabricated on back-contact photovoltaic cell. Sens. Actuat. B: Chem. 219 (2015) 43–49.
[21] L. Hu et al. An optimized ultraviolet-A light photodetector with wide-range photoresponse based on ZnS/ZnO biaxial nanobelt, Adv. Mater. 24 (2012) 2305-2309.
[22] Yin, Z. et al. Single-layer MoS_2 phototransistors. ACS Nano 6 (2012) 74–80.